

NOTES AND CORRESPONDENCE

Upper-Level Geostrophic Diffluence and Deepening of Surface Lows

FREDERICK SANDERS

Marblehead, Massachusetts

4 September 1992 and 19 January 1993

1. Introduction

A forecast rule, often cited prior to the advent of successful dynamical prediction, related deepening of surface cyclones to downstream spreading of upper-level height contours. The concept appears to have originated with Scherhag (1934). Bundgaard (1951) summarized Scherhag's statement of the rule as, ". . . cyclogenesis on the surface map usually occurs in those regions where, on an upper constant-pressure map, the absolute isohypses diverge. . . . On the surface map, frontal waves which move toward the exit (entrance) region [of an upper jet] will intensify (weaken)." The version of the rule by Oliver and Oliver (1945), as summarized by Dunn (1951), was that ". . . waves at the surface will deepen if the 700-mb contours diverge ahead of them," and will fill if they converge. More recently, Palmén and Newton (1969) assert that synoptic experience confirms the emphasis placed on the "diffluent upper trough." They cite Polster (1960) as finding that, "although initial wave formation took place in about one-fifth of the cases under confluent flow aloft, deepening under such flow was rare. By contrast, 73% of the cases of deepening cyclones were found under diffluent contours, predominantly ahead of upper troughs. . . ." Since the responsibility for prediction of surface cyclones has been largely assumed by the computer, the rule has lost its prominence, but occasional references to it can still be found.

The rule was advanced largely as a matter of empirical experience, and the only physical explanation offered was that this diffluence enhanced the upper-level evacuation, or divergence, of mass over the surface cyclone, leading to its intensification. Today this argument seems naive because, as Thaler (1992) has reiterated, diffluence is not tantamount to divergence. In nondivergent flow, for example, diffluence is exactly balanced by the downstream decrease of wind speed. Attempts have been made to tie diffluence to quasi-geostrophic theory by pointing to ascent and low-level convergent spinup in the left exit of a simple jet in

equivalent-barotropic flow, where diffluence is found. However, ascent is also favored in the right-rear jet entrance region, where there is confluence aloft and surface cyclones are also likely (hypothetically at any rate) to be deepening.

Thus, the rule is something of a mystery. The two questions that come to mind are, Is the rule true? and (if so) Why? A study was undertaken to answer these questions.

2. Some idealized patterns

It is not clear whether the rule refers to the broad-scale basic current on which an upper-level perturbation is superposed or on the total flow representing the sum of the basic current and the perturbation. To examine this question, we present some idealized flow patterns in Fig. 1.

Consider, at upper levels, a simple two-dimensional cyclonic perturbation superposed on a uniform broad-scale flow, as in Fig. 1a. The relative vorticity can be regarded as inversely proportional to the height perturbation. If the flow is approximately geostrophic, the height contours for the total flow are seen to be diffluent ahead of the trough, where there is cyclonic vorticity advection. A deepening surface cyclone will almost surely lie downstream from the upper perturbation, as shown. Note that such a cyclone lies under diffluent upper flow. Our understanding of this structure is based on the forcing of low-level convergence because of vorticity advection aloft. The diffluence is a natural structural aspect of the situation, without special physical significance.

The broad-scale upper flow, however, may not be uniform. In particular, it may display confluence or diffluence, or lateral shear in the cyclonic or anticyclonic sense. That is, the broad-scale flow may possess stretching or shearing deformation. If the same perturbation as in Fig. 1a is superposed on these idealized broad-scale flows, then the total flows are as illustrated in Figs. 1b–e. If the surface cyclone lies in the same position relative to the upper perturbation, then the cyclonic vorticity advection aloft is little altered but the contours are different. Over the surface cyclone they are more strongly diffluent if the broad-scale flow

Corresponding author address: Dr. Frederick Sanders, 9 Flint St., Marblehead, MA 01945.

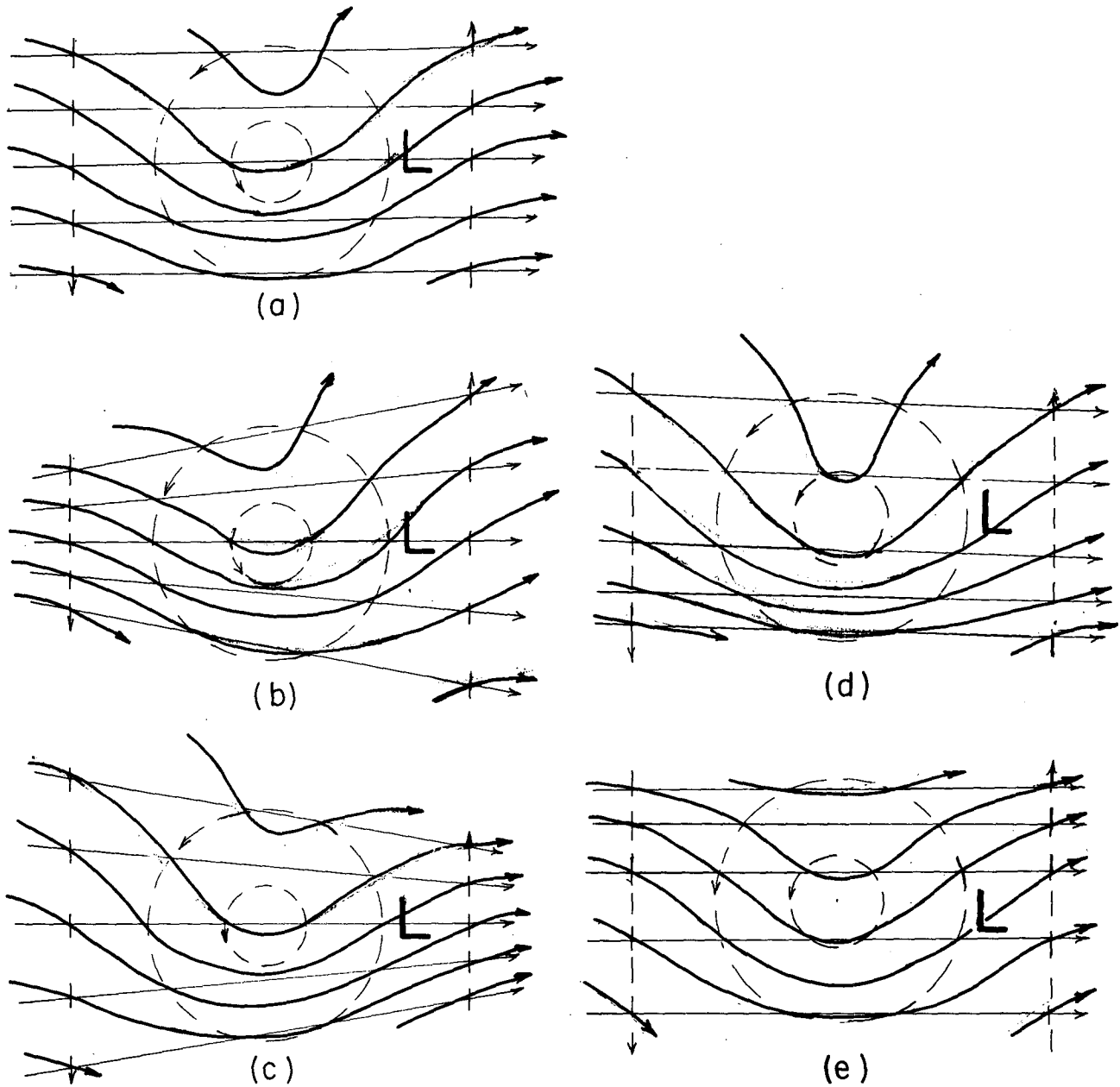


FIG. 1. Idealized upper-level height contour patterns resulting from superposition of a symmetric two-dimensional cyclonic disturbance (dashed lines) on various simple geostrophic basic currents (thin solid lines): (a) uniform, (b) diffluent, (c) confluent, (d) cyclonically sheared, and (e) anticyclonically sheared.

shows diffluence or cyclonic shear. If this flow possesses confluence or anticyclonic shear, the diffluence of the total flow over the surface cyclone is suppressed. It may in fact be confluent despite the cyclonic vorticity advection if the deformation is sufficiently intense relative to the strength of the perturbation.

A relationship of surface deepening to diffluence of the broad-scale flow would not be easy to interpret. A possible explanation was offered by Farrell (1989), who showed that a barotropic disturbance in a diffluent basic

current would grow provided it was initially elongated in the direction of the flow. With a greater height perturbation, such a more energetic upper-level disturbance might then be more effective in producing deepening of an associated surface cyclone. On the other hand, a disturbance elongated in a direction transverse to the basic current would grow in a confluent flow. Consideration of the aspect ratio of upper-level disturbances is beyond the scope of this note.

It is clear that our measurements of diffluence must

be made on the scale of the perturbation, and also on a larger scale. Only then can we determine if such a relationship (should it appear) is a matter of the internal structure of the disturbance, or if it refers to the large-scale flow.

3. The cyclone sample and methods of calculation

The regions and period selected for study were eastern North America and the central and western North Atlantic during the Experiment on Rapidly Intensifying Cyclones over the Atlantic (ERICA) field phase December 1988 through February 1989 (Hadlock and Kreitzberg 1988). Sanders (1992) has made a survey of surface cyclonic activity in this region and interval, as determined from the National Meteorological Center (NMC) operational manual analyses. Positions and central pressures of 40 individual low pressure systems were tabulated at 0000 and 1200 UTC during transit through the region. These data yielded 141 overlapping 24-h periods during which the deepening of a surface center was determined.

Diffuence and geostrophic advection of absolute vorticity were determined from the nested grid model (NGM) 500-mb analyses received on Difax. With the x axis taken along the direction of flow, stretching deformation is given by $\partial u/\partial x - \partial v/\partial y$, negative values denoting diffuence. In geostrophic flow with constant Coriolis parameter, $\partial u_g/\partial x = \sim \partial v_g/\partial y$, so that the deformation is expressed simply $2 \partial u_g/\partial x$. With the x axis similarly oriented, geostrophic vorticity advection is given by $-u_g \partial \eta/\partial x$.

Measurements of disturbance-scale deformation and absolute vorticity advection were made from the NGM 500-mb initial analyses by use of the square template illustrated in Fig. 2a. It was centered on the surface low and oriented along the 500-mb height contour above it. The finite-difference approximation for the deformation is then

$$\frac{2(u_6 - u_4)}{D} = \frac{2g}{f_0 D^2} [(Z_9 - Z_3) - (Z_7 - Z_1)], \quad (1)$$

where g and f_0 are the gravitational acceleration and the Coriolis parameter, and D was taken as 550 km, or 5° of latitude, as measured by dividers at the latitude of the cyclone. The corresponding expression for the vorticity advection is

$$\frac{g}{D^2 f_0} (Z_8 - Z_2)(\eta_4 - \eta_6), \quad (2)$$

where η is the absolute vorticity shown on the NGM initial analysis. In these calculations, the value of f_0 was taken at the latitude of the low center. These measurements could not be obtained for all cases in the sample, because some extended beyond the eastern limit of the NGM display area.

The broad-scale stretching deformation was obtained, from the hemispheric or "front-half" analyses,

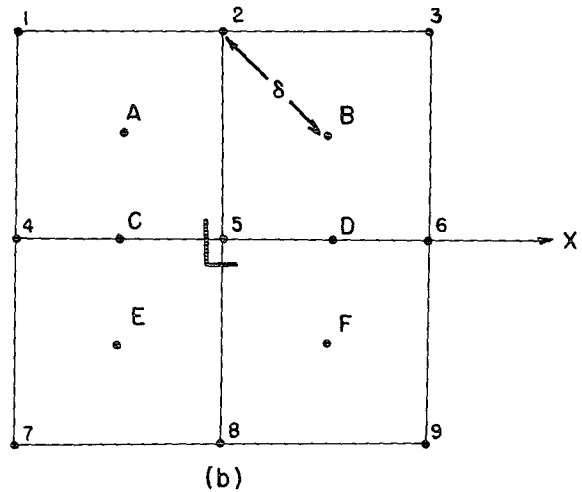
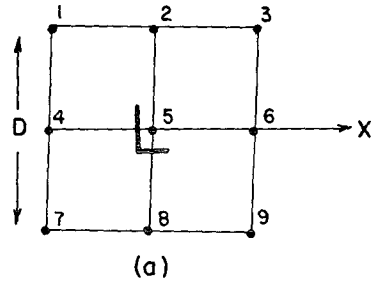


FIG. 2. Templates used for evaluation of stretching deformation and vorticity advection from 500-mb charts: (a) for disturbance scale with $D = 550$ km, and (b) for large scale, with $\delta = 660$ km. The x axis is oriented along the direction of the flow.

by applying the space-average technique introduced by Fj\o rtoft (1952), as a crude filter for removing the effect of the synoptic-scale disturbance. The application is illustrated by the template in Fig. 2b. The space-average 500-mb height at, say, point A (\bar{Z}_A) is the average of the heights at points 1, 2, 4, and 5. When the template is centered on the surface low and oriented along the direction of the large-scale geostrophic flow (estimated by making the sum of the heights at points 1 and 7 equal to the sum at points 3 and 9), then the broad-scale deformation is obtained by subtracting the speed of the space-average geostrophic flow at point C from that at point D . Again, the deformation is negative for diffluent flow. Since the speeds are determined by the differences of the space-average heights at points E minus A , and F minus B , respectively, the deformation is represented by

$$\frac{g}{4\delta^2 f_0} [(Z_9 - Z_3) - (Z_7 - Z_1)], \quad (3)$$

where the averaging distance, δ , was 660 km, as recommended by Fj\o rtoft (1952), measured on the map at latitude 45°N . (For convenience, the same template

was used at all latitudes, introducing small errors due to neglected variation of Coriolis parameter and map-scale factor.) This choice filters completely the horizontally two-dimensional wavelength of 2640 km.

The 24-h mean value of deformation or advection was obtained by averaging the value at the midtime with the mean of the values 12 h earlier and later.

4. Results and discussion

a. Disturbance scale

First, an attempt was made to verify the rule in the straightforward predictive sense, on the scale of the disturbance. That is, the sign of the stretching deformation on disturbance scale, aloft over the surface center at a given time, was compared with the sign of the central pressure change during the following 24 h. Instances of zero deformation were included with confluent cases, while instances of zero central pressure change were included with cases of filling lows. Results are shown in Table 1. It is seen that 69% of deepening lows (65 of 94) occurred with initial diffluence. The percentage increased slightly for the cases of more rapid pressure fall. Most lows deepened, however, so that deepening under confluent flow was not a rare event. Diffluent flow was present over the surface center in most of the cases, moreover, so that about half of the nondeepeners also occurred under diffluence.

These results are not inconsistent with those reported by Polster (1960), but close comparison is difficult, because in his study the scale on which the diffluence or confluence was evaluated was not specified. Further, his stratification of upper-level patterns included a substantial category of "parallel contour" cases, which was not specifically defined.

Use of deformation as a predictor in the present sample would have shown some small skill, since with diffluence 83% of lows deepened, while with confluence 71% did. By way of contrast, however, for 101 cases in which an NGM forecast was available for the range 0–24 h, forecast deepening was confirmed by the analyzed deepening 94% of the time, while the analyses showed deepening in only 21% of the instances in which the forecast did not. The NGM forecasts were substantially more skillful.

TABLE 1. Distribution-scale initial 500-mb stretching deformation and subsequent 24-h deepening of surface cyclones. Values in parentheses are percentages of column total.

	Diffluence	Confluence	Total
Deepening \geq 24 mb	18 (23)	7 (17)	25
Deepening \geq 15 mb	33 (42)	14 (34)	47
All deepening	65 (83)	29 (71)	94
Nondeepening	13 (17)	12 (29)	25
Total	78	41	119

In a diagnostic context, the signs of surface central pressure change and of concurrent 24-h mean deformation, for 100 cases in which all necessary values were available, were compared. Results were similar to those obtained with initial deformation, 82% of cases of diffluence and 73% of cases of confluence being accompanied by deepening.

The diagnostic relationship of surface deepening to disturbance-scale deformation and vorticity advection was further examined by calculating the linear correlation coefficients between 24-h mean values of these quantities themselves and between each, and 24-h deepening of the surface low. For 100 cases in which all the necessary quantities could be calculated, the average values of 24-h mean deformation, mean vorticity advection, and central pressure fall (with rms deviations in parentheses) were $-1.9(\pm 2.0) \times 10^{-5} \text{ s}^{-1}$, $+18(\pm 15) \times 10^{-10} \text{ s}^{-2}$, and $-12.1(\pm 14.2) \text{ mb}$, respectively.

The correlation coefficient between deformation and pressure change was only +0.30, while that between vorticity advection and pressure change was -0.57 . The latter magnitude would probably have been greater with representations of the vorticity fields that are smoother than those afforded by the NGM charts. That is, the patchiness of the vorticities suggests that the 24-h mean advection may not have been well represented by the use of data at 12-h intervals. It may be noted that the correlation coefficient between pressure change predicted by the NGM for the range 0–24 h and the analyzed change was +0.90, with an average predicted deepening of 10.4 mb. While this primitive equation model makes no explicit use of the vorticity advection, it is difficult to imagine how it could be so successful without confirming reasonably well the quasigeostrophic paradigm that relates this advection to deepening.

In any event, the correlation coefficient between 24-h mean stretching deformation and vorticity advection was -0.49 . We believe, therefore, that the underlying physical relationship is between deepening of a surface low and upper-cyclonic vorticity advection. The diffluent stretching deformation on disturbance scale is an imperfect proxy for this advection, reflecting the mixture of circulation types idealized in Fig. 1.

b. Large scale

We now examine deepening of surface centers in relation to stretching deformation on the large scale, for 143 cases. When the signs of the initial deformation and of central pressure change were compared, as seen in Table 2, the majority of all deepening cases occurred with confluent upper flow, contrary to Polster's (1960) result. The strongest deepeners, however, were favored by diffluent flow. Confluent cases were more frequent overall than diffluent ones, contrary to the results for the disturbance scale.

TABLE 2. As in Table 1 but for large-scale initial 500-mb stretching deformation.

	Diffluence	Confluence	Total
Deepening ≥ 24 mb	21 (41)	15 (16)	36
Deepening ≥ 15 mb	32 (63)	33 (36)	65
All deepening	46 (90)	73 (79)	119
Nondeepening	5 (10)	19 (21)	24
Total	51	92	143

Given the large-scale initial flow, deepening occurred in 90% of the cases with diffluence and 79% of those with confluence, indicating a small skill comparable to that shown by disturbance-scale initial flow. When the deepening was related to the concurrent 24-h mean large-scale upper deformation, as seen in Table 3, the preponderance of confluent flow was reduced, probably reflecting the tendency of many of the cyclones to move from a jet entrance to a jet exit region during the 24-h period. The implied predictive skill was also reduced, especially with respect to the strongest deepening category. The skill of either the initial or 24-h mean deformation as a predictor was no doubt smaller than the skill of the model forecast itself in prediction of sign of change of central pressure.

Examples of strong deepening of the surface cyclone with diffluent or confluent large-scale upper-level flow are shown in Figs. 3 and 4, respectively. The first represents a clear case of the diffluent upper trough at the middle of a 24-h period in which the stretching deformation was negative throughout. In the confluent case (Fig. 4), the deformation was strongly positive at the beginning and middle of the 24-h period, and approximately zero at the end, as the deepening surface cyclone rapidly traversed the jet entrance region.

The linear correlation between 24-h mean large-scale stretching deformation and change of central pressure was evaluated for the 141 cases. The mean deformation (and rms deviation) was $+0.007 (\pm 0.65) \times 10^{-5} \text{ s}^{-1}$, reflecting the majority of confluent cases seen in Table 3, while the mean pressure change (and rms deviation) was $-13.6 (\pm 14.0)$ mb. The correlation coefficient was $+0.17$, distinctly smaller than the value obtained for disturbance-scale deformation but still in the same sense. These results may be due to the effect of cyclonic vorticity advection on a scale large enough to survive

TABLE 3. As in Table 1 but for large-scale 24-h mean 500-mb stretching deformation and concurrent deepening.

	Diffluence	Confluence	Total
Deepening ≥ 24 mb	19 (30)	15 (19)	34
Deepening ≥ 15 mb	31 (49)	32 (41)	63
All deepening	55 (87)	62 (79)	117
Nondeepening	8 (13)	16 (21)	24
Total	63	78	141

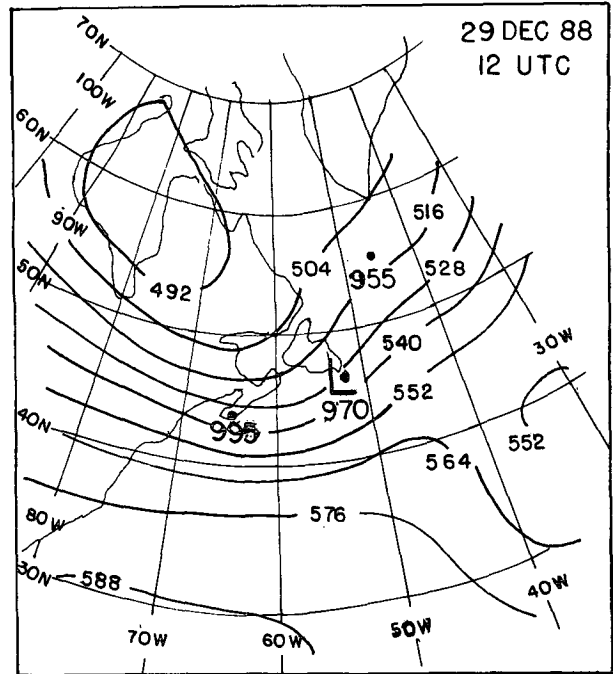


FIG. 3. Example of strong surface cyclogenesis with large-scale diffluence, 1200 UTC 29 December 1988. Solid lines are 500-mb contours at intervals of 12 dam. The solid dot denoted "L" shows the position of the surface low at this time, with central pressure in millibars. The other solid dots show the position of the low, annotated with central pressure, 12 h earlier and later.

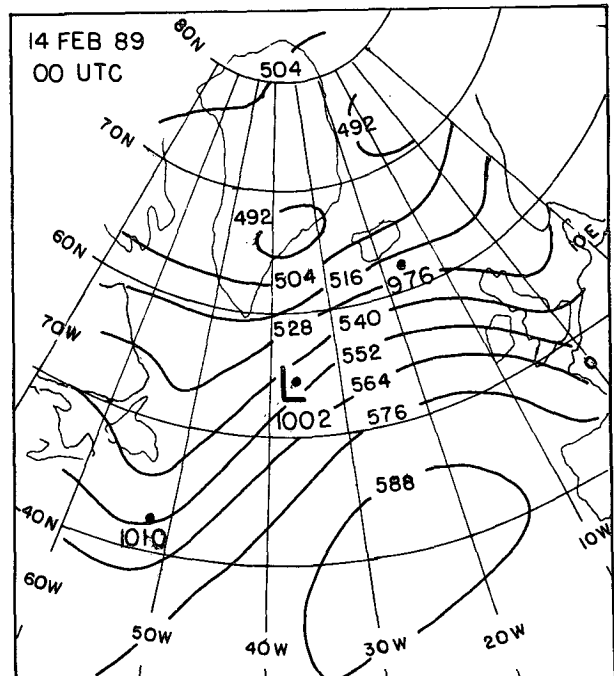


FIG. 4. Example of strong surface cyclogenesis with large-scale confluence, 0000 UTC 14 February 1989. Notation as in Fig. 3.

the filtering process used to estimate the broad-scale flow. The pattern in Fig. 3, for example, indicates a wavelength considerably larger than the 2640 km for which the space averaging was designed. An alternative possibility, that surface cyclogenesis is associated in some instances with barotropic growth of a favorably structured initial upper disturbance in diffluent or confluent flow, as described by Farrell (1989), was not examined.

5. Conclusions

For a sample of 40 cyclones over eastern North America and the western and central North Atlantic Ocean during the ERICA field phase December 1988–February 1989, only slight support was found for the empirical rule relating deepening of the surface low to downstream spreading of the upper-level contours over it. The relationship was less weak when the upper-level geostrophic diffluence was measured on the scale of the synoptic disturbance than when it was obtained from the larger-scale flow. Idealized flow patterns and calculations on disturbance scale support the view that the relationship is an imperfect reflection of the physical connection between surface deepening and cyclonic vorticity advection aloft. The explicit forecast of central pressure change by the dynamical model was a much better forecast than could be obtained by application of the rule.

This study, like Polster's (1960), was carried out in a region mainly oceanic with strong upward surface heat flux and frequent cyclogenesis. It is possible that the rule may work better elsewhere, in a region where there may be some synergistic relationship between upper diffluence and the effects of the earth's surface. This possibility was not examined.

The relative success of the dynamical model does not mean that its forecast cannot be improved upon,

only that a diffluent pattern aloft is not a good basis. A knowledge of systematic error, consistency of successive forecasts, and close surveillance of observations subsequent to model initialization are more likely bases.

Acknowledgments. This research was supported by the Office of Naval Research under Contract N00014-91-C-0241. The author is grateful to the Center for Meteorology and Physical Oceanography, Massachusetts Institute of Technology, for furnishing facilities and materials; to Isabelle Kole for drafting the figures; and to Lars Schade for assistance in translation.

REFERENCES

- Bundgaard, R. C., 1951: A procedure of short-range weather forecasting. *Compendium of Meteorology*, T. F. Malone, Ed., Amer. Meteor. Soc., 766–795.
- Dunn, G. E., 1951: Short-range weather forecasting. *Compendium of Meteorology*, T. F. Malone, Ed., Amer. Meteor. Soc., 747–765.
- Farrell, B. F., 1989: Transient development in confluent and diffluent flow. *J. Atmos. Sci.*, **46**, 3279–3288.
- Fjørtoft, R., 1952: On a numerical method of integrating the barotropic vorticity equation. *Tellus*, **4**, 179–194.
- Hadlock, R., and C. W. Kreitzberg, 1988: The experiment on rapidly intensifying cyclones over the Atlantic (ERICA) field study: Objectives and plans. *Bull. Amer. Meteor. Soc.*, **69**, 1309–1320.
- Oliver, V. J., and M. B. Oliver, 1945: Forecasting the weather with the aid of upper-air data. *Handbook of Meteorology*, F. A. Berry, Jr., E. Bollay, N. R. Beers, Eds., McGraw, 813–857.
- Palmén, E., and C. W. Newton, 1969: *Atmospheric Circulation Systems*. Academic Press, 334–335.
- Polster, G., 1960: Über die Bildung und Vertiefung von Zyklonen und Frontwellenentwicklungen am konfluenten Hohentrog. *Meteorol. Abhandl., Inst. Meteorol. Geophys. Bioklimatol.*, **A14**, 1–70.
- Sanders, F., 1992: Skill of operational dynamical models in cyclone prediction out to five-days range during ERICA. *Wea. Forecasting*, **7**, 3–25.
- Scherhag, R., 1934: Zur Theorie der Hoch- und Tiefdruckgebiete. *Meteor. Z.*, **51**, 129–138.
- Thaler, E., 1992: Divergence and diffluence are not synonyms. *Natl. Wea. Dig.*, **17**, 28–29.